

Molecular orbital calculations on $[\text{HRu}_3(\text{CO})_9(\text{PhNCO})]^-$ and related clusters

SUMIT BHADURI*^{†a}, ABHIJIT CHATTERJEE^b, SOURAV PAL*^b,
SHILPA TAWDE^a and DOBLE MUKESH^a

^aAlchemie Research Centre, P O Box 155, Thane-Belapur Road, Thane 400 601, India

^bNational Chemical Laboratory, Pune 411 008, India

[†]Present address: ACC, Research and Consultancy Directorate, CRC Complex, LBS Marg, Thane 400 604, India

MS received 23 August 1995; revised 2 September 1996

Abstract. Molecular orbital calculations (EHMO) have been performed on five ruthenium carbonyl clusters considered to be involved in the reductive carbonylation of nitrobenzene. The bonding in the isocyanate cluster, $[\text{HRu}_3(\text{CO})_9(\text{HNCO})]^-$, is shown to arise mainly from the interaction between the LUMO of HNCO and HOMO of the $[\text{HRu}_3(\text{CO})_9]^-$ fragment. The relative stabilities of this cluster, two of its isomers and the CO-eliminated cluster $[\text{HRu}_3(\text{CO})_9(\text{HN})]^-$, are also commented upon. The calculated results are in accordance with empirical kinetic data.

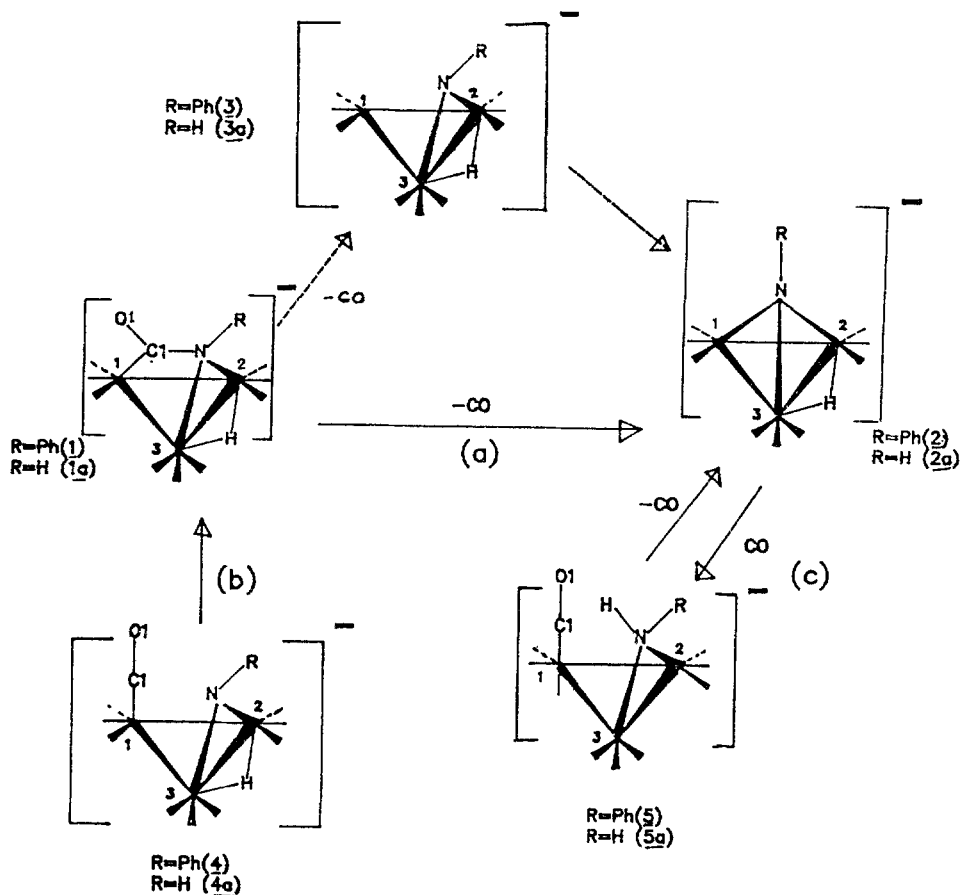
Keywords. Ruthenium carbonyl clusters; extended Hückel MO calculations; reductive carbonylation of nitrobenzene.

1. Introduction

Reductive carbonylation of nitrobenzene with $\text{Ru}_3(\text{CO})_{12}$ as a homogeneous catalyst is a well-studied reaction (L'Eplattenier *et al* 1970; Alper *et al* 1978, 1980, 1981; Cenini *et al* 1984; Basu *et al* 1987; Bhaduri *et al* 1990). A number of reaction steps and the structures of the associated clusters have been fully established (Williams *et al* 1985, 1987; Bhaduri *et al* 1988, 1989, 1990). The ones relevant to the work described in this paper are shown in scheme 1. The cluster $[\text{HRu}_3(\text{CO})_9(\text{PhNCO})]^-$ (**1**), where a phenyl isocyanate ligand is bound to the metal triangle in a μ_3 fashion, is considered to play an important role as a catalytic intermediate (Bhaduri *et al* 1989, 1990). As shown in scheme 1, reaction (a), under ambient conditions this cluster undergoes facile loss of carbon monoxide with the formation of $[\text{HRu}_3(\text{CO})_9(\text{PhN})]^-$ (**2**); reaction (b) is the proposed mechanism for the formation of (**1**) from an anionic precursor $[\text{HRu}_3(\text{CO})_{10}(\text{PhN})]^-$ (**4**). Cluster (**4**) is isoelectronic with (**1**) and has another isomer $[\text{Ru}_3(\text{CO})_{10}(\text{PhNH})]^-$ (**5**). This cluster, where the bridging hydrogen moves onto the nitrogen atom, is formed in a reversible manner by the carbonylation of (**2**). Cluster (**5**) cannot be isolated as a solid but has been adequately characterised in solution by spectroscopic data. Clusters (**1**) and (**2**) have been characterised by single crystal X-ray structure determinations.

Thus, of the five species shown in scheme 1, three are fully characterised, while the involvement of the other two, (**3**) and (**4**), as intermediates is more than likely. In this

*For correspondence



paper we describe extended Hückel molecular orbital calculation results on (1a)–(5a). In particular, we probe the nature of the bonding between the isocyanate functionality and the trinuclear metal fragment. We also evaluate the extent to which theoretical findings are in accordance with kinetic results and the observed reactivity of (1).

2. Results and discussion

Molecular orbital calculations were performed using the extended Hückel program (HP Version 1989) of Hoffmann and coworkers at the Cornell University, Ithaca. Eigenvectors, eigenvalues, Mulliken overlap populations between atoms and the net charges on them were computed with the mean Wolfsberg–Helmholtz formula. The extended Hückel parameters were taken from Pilcher and Skinner (1962) and Zerner and Guterman (1966).

Bond distances and angles as determined by X-ray structural data of (1) and (2) have been used for the calculations. To reduce the size of calculations, model complexes (2a)–(5a) rather than (2)–(5) have been studied. By carrying out calculations on (1) and

comparing the results with those for (1a), it has been verified that the qualitative bonding descriptions and the trends associated with the structural changes remain the same for both these classes of complexes.

The ligand PhNCO has different geometries in the free state and in the coordinated state. In the free state, on the basis of spectroscopy, a near-linear NCO group and a Ph-N-C angle approximately equal to 141° have been proposed (Patai 1977). For HNCO the HNC angle is found to be 128° while the NCO group is thought to be linear. In (1) however, both Ph-N-C and NCO angles are very close to 120° .

As shown in the Walsh-type diagram of figure 1, the main effect of bending the NCO angle from 180° to 120° is to mix the lowest unoccupied molecular orbital (LUMO) $3a'$ and the occupied molecular orbital $2a'$. This substantially lowers the energy of $3a'$ which is strongly CO antibonding and weakly C-N bonding. Bending the N-C-O

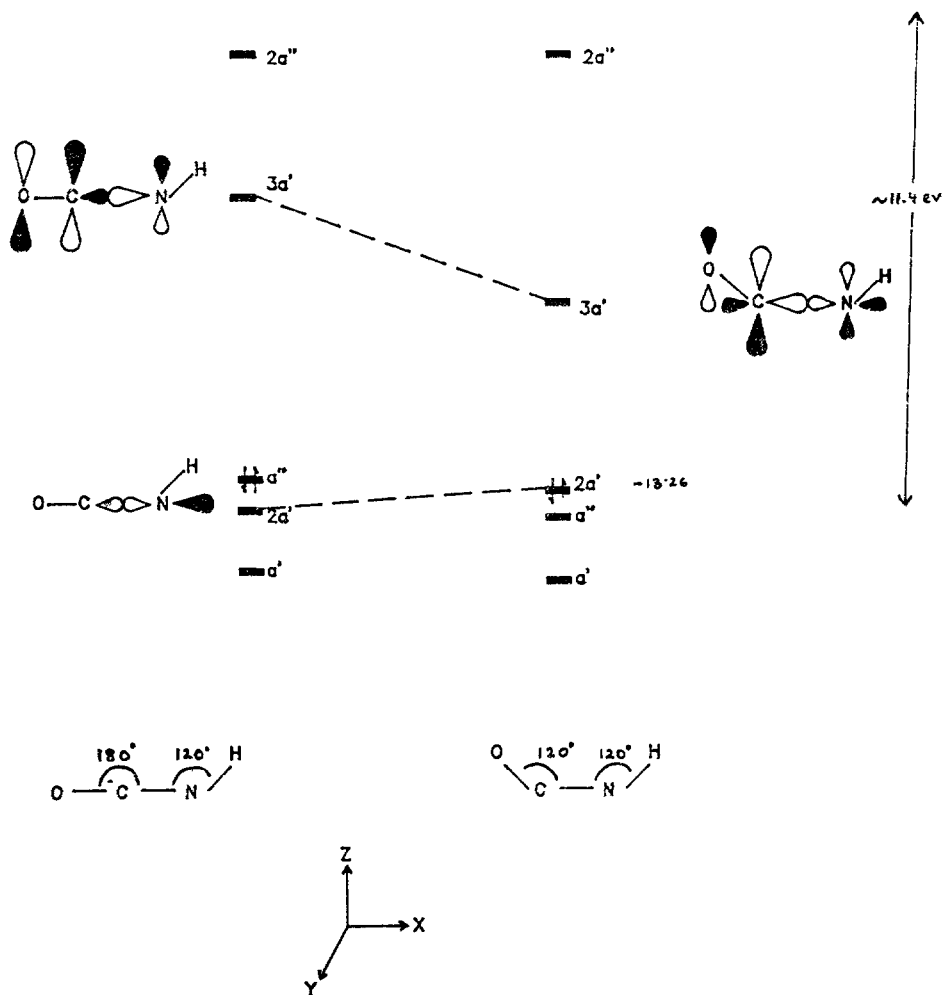


Figure 1. Walsh diagram for bending O-C-N angle of HNCO from 180° to 120° . Energy scale approximate.

angle also lifts the energy of the $2a'$ orbital slightly, so that it becomes the highest occupied molecular orbital (HOMO). How the lowering of the energy of $3a'$ helps bond formation in (1a) will be seen shortly.

The molecular orbitals of (1a) may be constructed from those of symmetrically bent HNCO and those of $[\text{HRu}_3(\text{CO})_9]^-$ (6) (figure 2, bottom). Alternative ways of constructing these orbitals, discussed later, are perhaps less useful since they do not explicitly discuss HNCO or PhNCO as ligands. Schilling and Hoffmann's classic analysis of the " $\text{M}_3(\text{CO})_9(\text{ligand})$ " system may be used as a starting point to gain

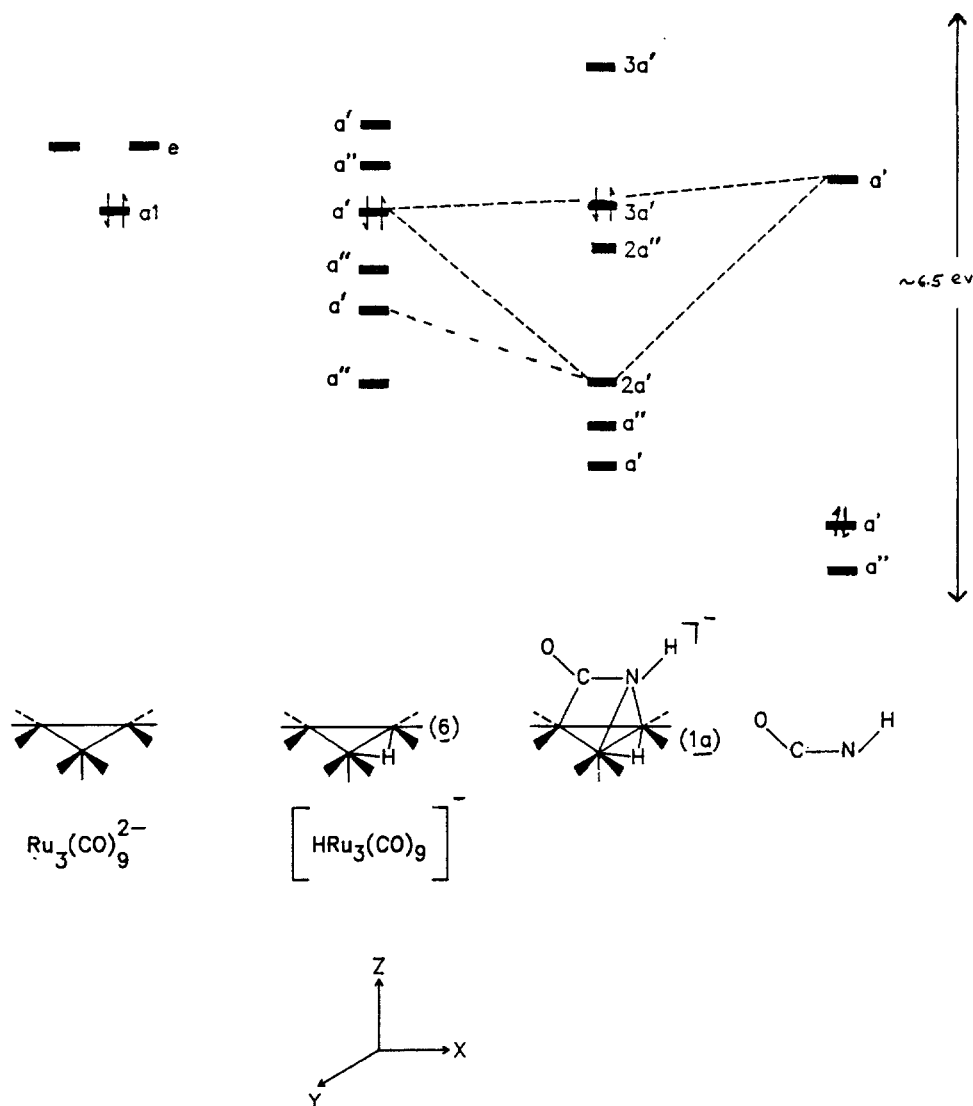


Figure 2. Interaction diagram for the construction of the MOs of (1) from smaller fragments $[\text{HRu}_3(\text{CO})_9]^-$ and symmetrically bent HNCO. Energy scale approximate.

qualitative insight (Schilling and Hoffmann 1979). Cluster (1a) is isoelectronic with $[\text{Ru}_3(\text{CO})_9(\text{HNCO})]^{2-}$ and the molecular orbitals of this species may be constructed from those of $\text{Ru}_3(\text{CO})_9^{2-}$ and the symmetrically bent HNCO.

The orbital diagram of $\text{Ru}_3(\text{CO})_9^{2-}$ may be assumed to be that of " $\text{Fe}_3(\text{CO})_9$ " with two extra electrons. The lowest unoccupied frontier orbitals of this molecular fragment of C_{3v} symmetry have been shown to consist of a low-lying a_1 , and a degenerate 'e' pair. In $\text{Fe}_3(\text{CO})_9^{2-}$ the a_1 orbital is the HOMO. From a separate calculation on (6) we find that lowering of symmetry from C_{3v} to C_s lifts the degeneracy of the e orbital slightly but leaves the relative ordering of the HOMO (a') and the other two orbitals unaltered. The molecular orbitals of (1a) as constructed from HNCO and (6) are shown in figure 2.

The HOMO of (1a), $3a'$, is weakly bonding with respect to the N-C bond and the Ru2-N-Ru3 interaction. However, it is weakly antibonding with respect to C1-O1 and Ru1-C1 interactions. The important orbital interactions are shown schematically in (7). The next filled orbital, $2a''$, is essentially non-bonding with some C1-O1 antibonding character. The main stabilising interaction associated with $2a'$ arises mainly from the LUMO of HNCO and the top two occupied orbitals of a' symmetry of (6). It may be recalled that the symmetrical bending of HNCO substantially lowers the energy of its LUMO (figure 1). The bending of the ligand is thus necessary for making the bonding interaction possible and favourable. Orbital $2a'$ is strongly bonding with respect to the interaction between the carbon atom and Ru1, on the one hand, and weakly bonding with respect to Ru2-N-Ru3 interaction, on the other. It is also bonding with respect to the interaction between the carbon and nitrogen atoms. The low symmetry of 1a causes extensive mixing of orbitals of a given symmetry type.

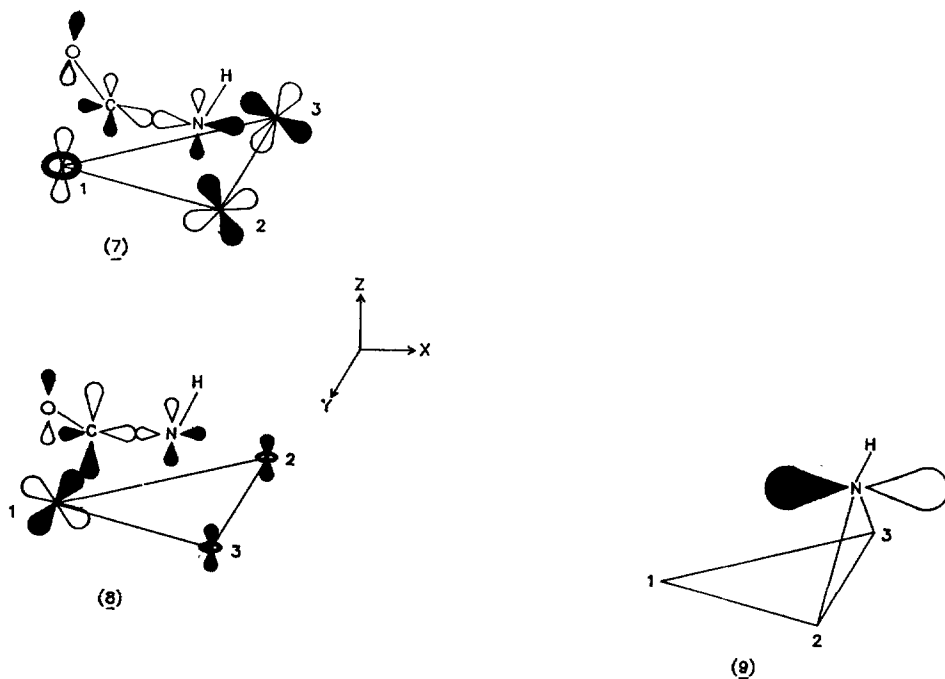


Table 1. Selected computed parameters of (1a)–(5a).

Cluster	Sum of one-electron energy (eV)	HOMO, LUMO energies (eV)	Net charge on nitrogen carbon	Reduced overlap population
(1a)	– 2458.63	– 9.54 – 8.01	– 0.22 0.69	Ru1–C1 0.6, Ru2–N 0.31, Ru3–N 0.31, C1–N 0.97 C1–O 1.1
(2a)	– 2264.76	– 10.06 – 7.84	– 0.56	
(3a)	– 2261.39	– 9.83 – 8.98	– 0.89	
(4a)	– 2459.86	– 9.29 – 7.97	– 1.0 0.65	
(5a)	– 2459.99	– 9.54 – 7.97	– 0.31 0.73	

Consequently $2a'$ has contributions from both the high-lying orbitals of a' symmetry of (6). The important orbital interactions are shown schematically in (8).

The reduced overlap population for selected bonds in (1a) is given in table 1. The bond-orders of all the bonds between HNCO and (6) are less than one. The C1–N bond order is indicative of a single bond consistent with the structural data.

The molecular orbitals of (1a) could also be constructed from those of "HRu₃(CO)₉(HN)" (3a) and CO, or "HRu₃(CO)₁₀" and "(HN)". The molecular orbital scheme of "HM₃(CO)₁₀" has recently been reported (Jemmis and Prasad 1991). While both these approaches give the same results, the former is more informative for two reasons. First, mechanistic studies indicate possible involvement of a (4) like transition state in the conversion (1) to (2). Secondly, it allows a comparison to be made between isoelectronic (3a) and (2a), structures that are different from each other mainly in terms of Ru1–N distance.

The molecular orbital scheme of (3a), easily constructed from (6) and "HN" or by removing the C101 from (1a), is shown in figure 3. The HOMO of a'' symmetry is essentially a non-bonding orbital very similar to $2a''$ of (1a) (see figure 1) and located mainly on Ru1. The LUMO of a' symmetry, schematically shown by (9), has large contributions from the nitrogen p_x . The interaction between the donor HOMO of a' symmetry on CO and mainly this empty orbital of (3a) leads to the already discussed, $2a'$ of (1a) (also see figure 1). Here again the low symmetry of (3a) leads to contribution from the high-lying occupied orbital of a' symmetry. The interaction diagram constructed this way reveals the reason for the relatively easy loss of C101 from (1) to give (2) (scheme 1, reaction (a)). From figure 3 it is apparent that there is very little or no stabilisation of C101 on bond formation with (3a).

In going from structure (3a) to (2a), the energies of the high-lying occupied orbitals change very little. The main stabilising and bonding interaction between the nitrogen and the three ruthenium atoms comes from a deep-lying occupied orbital (not shown)

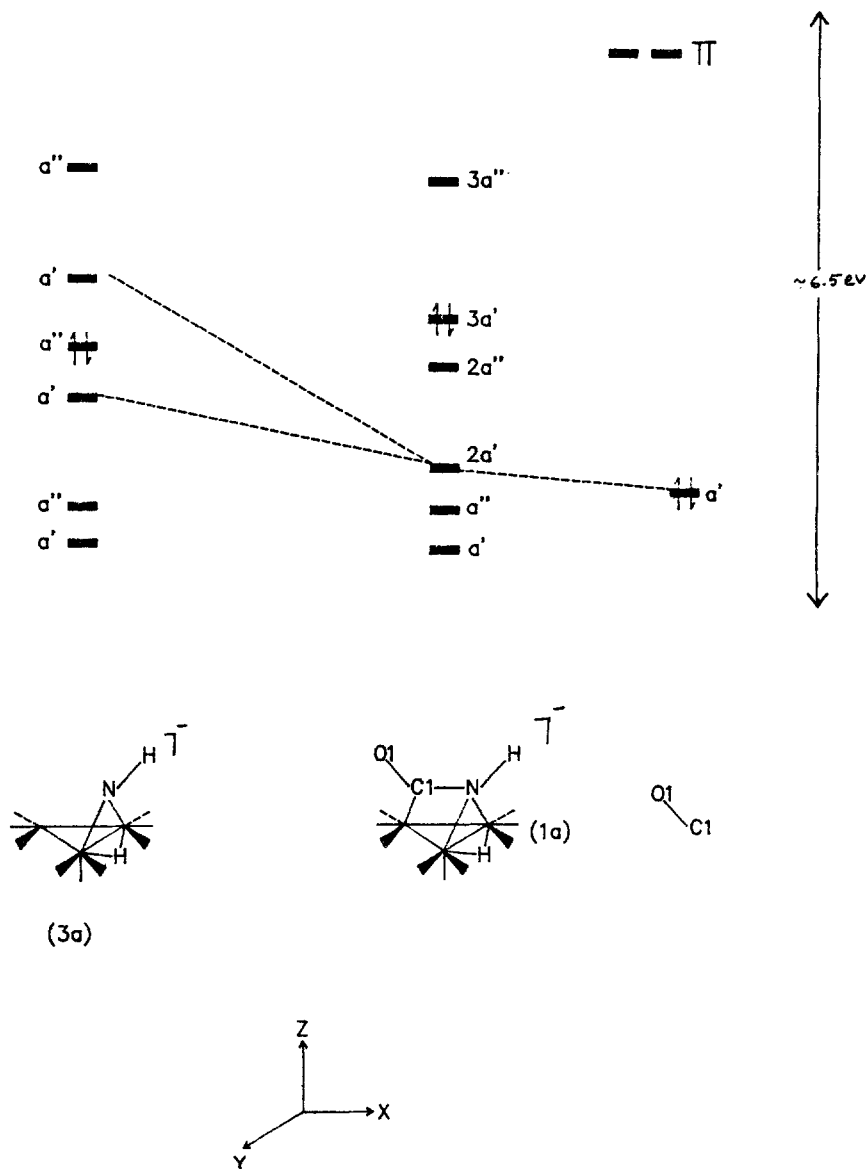


Figure 3. Molecular orbital scheme of (1a) constructed from the interaction diagram of $[\text{HRu}_3(\text{CO})_9(\text{NH})]^-$ and CO. Energy scale approximate.

composed mainly of the nitrogen p_z and the ruthenium d_{z^2} orbitals. Bonding in similar complexes has been discussed in detail by Schilling and Hoffmann (1979). The LUMO of (2a) is substantially destabilised and the HOMO-LUMO gap is 2.22 eV (table 1) as opposed to 0.85 eV in (3a). The sums of the one-electron energies for (3a) and (2a) are -2261.4 and -2264.8 eV respectively. On theoretical considerations (3a) would thus be expected to convert to the more stable structure (2a).

Structures (4a), (5a), and (1a), though isoelectronic, differ from each other in terms of C1 to nitrogen distance, the orientation of the C1O1 group and the distance between the nitrogen and the bridging hydrogen atom. As shown in table 1, these structural changes have little effect on the energies of the frontier orbitals. The sum of the one-electron energies of (1a), (4a) and (5a) is almost the same.

Removal of a proton from the amido group in the structurally characterised cluster $\text{HRu}_3(\text{CO})_{10}(\text{NHR})$ ($\text{R} = \text{Ph}$), leads to the formation of (4). The HOMO of (4a) is expected and found to be located mainly on the nitrogen atom. In (5a) the HOMO has a smaller contribution from the nitrogen and, as the formal valence bond structure indicates, is bonding with respect to nitrogen and hydrogen with approximately equal contributions from these two atoms. The net negative charge on the nitrogen atom in (5a) is therefore expected to be much lower as is indeed the case.

It may also be noted (table 1) that the net negative charge on the nitrogen and the positive charge on C1 in (4a) are noticeably higher than those in (1a). The intramolecular nucleophilic attack by nitrogen onto the coordinated CO in (4a) (scheme 1, reaction (b)) is therefore expected. The high negative charges on the nitrogen atom in (3a) and (4a) are also in agreement with the results of a Hammett plot for reaction (a). Such a plot indicates negative charge accumulation on the nitrogen in the transition state.

From empirical kinetic measurements, the ΔG^\ddagger for the conversion of (1) to (2) has been estimated to be $\approx 84 \text{ kJ mol}^{-1}$ i.e. 0.87 eV (Bhaduri et al 1990). In table 1 the sum of one-electron energies of clusters (1a)–(5a) is shown. It is clearly recognised that these values are at best very approximate and that electronic energy is only one of the many contributing terms to the total free-energy of a system. However, as a first and crude approximation, the sum of one-electron energies may be taken as an indicator of thermodynamic stability. In terms of one-electron energies, that of (1a) is about 120 to 130 kJ less than those of (4a) and (5a). The stability of (1) with respect to spontaneous change to (4) or (5) would thus appear to be kinetic in nature. It is interesting to note that carbonylation of (2) leads to (5) rather than (1). Assuming the kinetic barriers of both the carbonylation routes to be of similar magnitude, formation of (5) is expected in view of its lower one-electron energy i.e. thermodynamic stability.

Acknowledgement

Professor R Hoffmann very kindly allowed us to use his EHMO program, Mr A B Mandhara assisted with the computation, and ICI, India and the Council of Scientific and Industrial Research, New Delhi provided financial support for this work. We thank one of the referees for pointing out an error in the earlier version of this paper.

References

- Alper H and Amaratunga S 1980 *Tetrahedron Lett.* **21** 2603
- Alper H and Hashem K E 1981 *J. Am. Chem. Soc.* **103** 6514
- Alper H and Paik N H 1978 *Nouv. J. Chim.* **2** 245
- Basu A, Bhaduri S and Khwaja H 1987 *J. Organomet. Chem.* **319** C28
- Bhaduri S, Khwaja H and Jones P G 1988 *J. Chem. Soc., Chem. Commun.* 194
- Bhaduri S, Khwaja H, Sharma K and Jones P G 1989 *J. Chem. Soc., Chem. Commun.* 515
- Bhaduri S, Khwaja H, Sapre N, Sharma K, Basu A, Jones P G and Carpenter G 1990 *J. Chem. Soc., Dalton Trans.* 1313
- Cenini S, Pizzotti M, Crotti C, Porta and La Monica G 1984 *J. Chem. Soc., Chem. Commun.* 1286

- Jemmis E D and Prasad B V 1991 *Organometallics* **10** 3613
L'Eplattenier F, Matthys P and Calderazzo F 1970 *Inorg. Chem.* **9** 342
Patai S (ed.) 1977 *The chemistry of cyanates and their thio derivatives, Part 1* (New York: John Wiley and Sons) p. 82
Pilcher G and Skinner H S 1962 *J. Inorg. Nucl. Chem.* **24** 1937
Schilling B E R and Hoffmann R 1979 *J. Am. Chem. Soc.* **101** 3456
Williams G D, Geoffroy G L, Whittle G L and Rheingold A L 1985 *J. Am. Chem. Soc.* **107** 729
Williams G D, Whittle R R, Geoffroy G L and Rheingold A L 1987 *J. Am. Chem. Soc.* **109** 3936
Zerner M and Gutterman M 1966 *Theor. Chim. Acta* **4** 44